APPLIED PHYSICS

***An electrostatic field mill (EFM) is widely used to measure the strength of electrostatic fields, the main drawback of which is the occurrence of large measurement errors (up to 15 % in the range from 0 to 1 kV/m).***

***This paper examines the aspects of using transimpedance amplifiers (TIAs) for the tasks of converting the current received from the EFM sensor into voltage, which will make it possible to reduce the instrumental error and ensure the linearity of the atmospheric electrostatic field strength measurement. In the general case, for the functional circuits of the electrostatic field mill, which include a differential transimpedance amplifier, there is the use of two TIA circuits, which are connected in parallel. Despite the simplicity of implementation, such a configuration contains a number of disadvantages and is not optimal. In the paper, a comparative analysis of a typical circuit of a differential TIA and a circuit of an ungrounded differential transimpedance amplifier with zero voltage drop proposed by the authors is carried out.***

***As a result of the analysis, it was established that the designed authentic circuit of the ungrounded differential transimpedance amplifier with zero voltage drop has better parameters of linearity and interference resistance, in contrast to the generally accepted one. The value of the signal-to-noise ratio for the proposed scheme improved by 42 % on average compared to the typical one. The main difference of the proposed scheme is that the stability of the amplification factor is ensured, the influence of the bias parameters of the operational amplifier is leveled, and the overall noise level is reduced. The use of the designed scheme of an ungrounded differential transimpedance amplifier with zero voltage drop could make it possible to increase the accuracy of the measurement of the electrostatic field strength***

***Keywords: atmospheric electric field, electrostatic field strength, electrostatic field mill, transimpedance amplifier***

UDC 621.3.082.72
DOI: 10.15587/1729-4061.2023.292691

# INCREASING THE ACCURACY OF ELECTROSTATIC FIELD STRENGTH MEASUREMENT BY USING AN IMPROVED DIFFERENTIAL TRANSIMPEDANCE AMPLIFIER CIRCUIT

**Oleksandr Povshenko**
*Corresponding author*
Postgraduate Student
Department of Information and Measuring Technologies*
E-mail: scela2472@gmail.com
**Viktor Bazhenov**
PhD, Associate Professor
Department of Automation and
Non-Destructive Testing Systems*
**Olha Pazdrii**
Assistant
Department of Computer-Integrated
Optical and Navigation Systems*
**Halyna Bohdan**
PhD, Associate Professor*
Department of Automation and
Non-Destructive Testing Systems*
*National Technical University of Ukraine
«Igor Sikorsky Kyiv Polytechnic Institute»
Beresteiskyi (Peremohy) ave., 37, Kyiv, Ukraine, 03056

*Received date 12.10.2023*
*Accepted date 14.12.2023*
*Published date 29.12.2023*

***How to Cite:*** *Povshenko, O., Bazhenov, V., Pazdrii, O., Bohdan, H. (2023). Increasing the accuracy of electrostatic field strength measurement by using an improved differential transimpedance amplifier circuit. Eastern-European Journal of Enterprise Technologies, 6 (5 (126)), 6–14. doi: https://doi.org/10.15587/1729-4061.2023.292691*

## 1. Introduction

The atmospheric electrostatic field is created by a potential difference of about 250 kV between the electrically conductive ionosphere and the Earth, which results from the separation of charges in thunderstorm clouds. The key parameter of atmospheric electricity is the intensity of the electric field. In good weather, the typical electric field strength in an open flat area at ground level is about 100 V/m, and at an altitude of several kilometers already 20–30 V/m. However, local weather conditions, such as charged thunderstorm clouds, can cause significant changes in the local electric field, resulting in values of several kV/m or even 100 kV/m on high mountain tops.

The main device for measuring such fields is an electrostatic field mill [1–3]. Electrostatic field mill (EFM) is an electrometer of variable capacitance, that is, it measures the local ambient electric field in place due to the charge accumulated on the surface of the measuring plate. It is widely used for monitoring electric fields under adverse environmental conditions:

– in meteorology to study the occurrence of thunderstorms [4–6];

– in lightning warning systems to protect material assets [7, 8];

– to control the electrostatic field on large oil tankers [9];

– to study electric fields near high-voltage power lines and other electrical equipment [10].

One of the important requirements for on-board EFMs is the measurement of small values of electric field strength (of the order of 1 V/m) [11]. After all, the measurements of the signals associated with the calibration maneuvers of the aircraft are performed in good weather, preferably cloudless. The main disadvantage of EFM is rather large errors in measuring the strength of the electrostatic field strength (EFS) (up to 15 % in the range from 0 to 1 kV/m), the occurrence of which is associated with the imperfections of the mathematical model and outdated hardware [12]. The decisive quantitative parameter that characterizes the quality of the measurement system is the signal/noise ratio. To improve the value of this system parameter, it is necessary to increase the value of the usable signal and reduce the mean square value of the total noise. One way to increase the usable signal is to improve the sensitivity of the sensor.

For the vast majority of known EFM functional circuits, which include a differential transimpedance amplifier (TIA) [4, 11, 13–16], a typical solution is the use of two TIA circuits that are connected in parallel, each of which is intended for a separate group of plates, outputs which are fed to the differential amplifier. Despite the simplicity of such an implementation, it contains a number of inherent disadvantages of TIA and is not optimal. The main disadvantages of such a scheme include the instability of the amplification factor, the large influence of the bias current on the shift of the output signal, and the high level of general noise against the background of which it is difficult to distinguish the signals of small currents.

Therefore, it is a relevant task to investigate the improvement of TIA circuits in order to increase the signal-to-noise ratio during the measurement of small values of the EFM current.

## 2. Literature review and problem statement

In [4], the results of research on high-speed, autonomous EFMs for the study of thunderstorms are given. This paper proposes a ground-based EFM design in which the currents induced on both sets of electrodes are amplified by means of independent TIAs. In turn, TIAs are connected to the differential inputs of the variable gain amplifier (VGA) via capacitive coupling. Using this configuration provides level shifting and adjustable gain. Also, the advantage of the study reported in [4] is the description of the sequence of data processing and calibration of the device.

The disadvantage of work [4] is that the numerical value of the measurement accuracy of the proposed device was not presented. Questions related to the calculation of the actual measurement error of the given scheme remained unresolved. The given value of the EFM resolution of 2 V/m per lower digit does not demonstrate the actual value of the EFM measurement error since the presence of noises that make up at least 3 lower device digits was not taken into account. To demonstrate the effectiveness of the proposed EFM, it is advisable to calculate the noise characteristics of the circuit to determine the effective number of bits (ENOB) parameter.

Study [12] gives the results of studies of EFM with a low noise level and internal digitization for on-board platforms. The EFM described in the paper is very sensitive (1 V/m per 1 bit), has a wide dynamic range (115 dB) and a very low noise level (1 LSB). These aircraft-mounted EFMs can measure fields from 1 V/m to 500 kV/m. The device uses 16-bit A/D converters, which provides maximum field sensitivity of 63.6 kV/m (sensitive) and 1.15 MV/m (insensitive) channels.

It is shown that the device has a wide dynamic range of 115 dB (~19.1 bit), but there are still unsolved questions, due to which it is provided. The numerical value of the sensitivity of the sensor used in the device was also not presented. An option to overcome these difficulties may be to provide a more detailed description of the method of calculating the errors of the electrical path of the device and a description of the software implementation of the processing of signals received from the sensor.

Paper [13] reports a highly sensitive microelectromechanical EFM based on torsional resonance. The proposed device uses a torsion gate, which consists of shielding electrodes and torsion beams. Movable shielding electrodes and fixed sensitive electrodes are made on the same plane. It is shown that the device works in the range from 0–50 kV/m. As a result of the experiment, a linearity of 0.15 % was established, and the error was below 0.38 % in three consecutive measurements.

Among the advantages of the cited study is a high sensitivity of 48.2 fA/(V/m), which was achieved with the help of a high frequency of torsional resonance. Along with this, study [13] has a number of remarks, which include the fact that the calculated sensitivity of the sensor takes into account the amplification factor of the TIA, which is not part of the microelectromechanical EFM. Also, the noise characteristics of this tract are not presented. The determination of the measurement error in the work is based on a small sample of data, and the method of conducting the experiment is only partially described. An option to overcome these difficulties may be the inclusion of TIA noise in the calculation of the total error of the microelectromechanical EFM. It would also be advisable to conduct more experiments and increase the number of readings on the measuring range.

In [14], two operational amplifiers (OAs) with a low-power 3 V cascade amplifier were compared in order to choose the most suitable one for the preamplification stage of the electric field sensor.

It is shown that after optimizing the noise of both operational amplifiers, the OA pmos can have half the silicon area of a rail-to-rail OA, while demonstrating the same noise characteristics. But the issues related to the configuration of TIA to optimize the noise of the circuit remained unresolved. An option to overcome the relevant difficulties can be a review of the design parameters that should be taken into account in the process of designing a sensor interface for an electric field mill. As well as the development of new TIA configuration solutions that will reduce its overall noise level. This is the approach used in works [15, 16], however, not all variants of the implementation of the differential TIA scheme were considered, which make it possible to reduce the level of general noise, thereby increasing the sensitivity of electrostatic field sensors.

In [17], the results of research aimed at increasing the accuracy of EFS measurement are given. The authors proposed the use of a universal mathematical model of the EFM sensor and considered the components that affect its sensitivity. It also presented its own generalized functional scheme of the EFM for which the method of calculating the instrumental error was described.

Based on the mathematical model of the sensor presented in [17], the dependence of the current change for a typical

EFM sensor was established. Also reported was the methodology for calculating TIA noise, which made it possible to determine the approximate value of the rms voltage of the noise of amplifiers. As a result of the analysis of the obtained values, it was established that the main component of the instrumental error in the EFM occurs at the stage of converting the current from the sensor into voltage. But questions related to the methods and means of reducing the impact of TIA noise on the sensitivity of the EFM sensor remained unresolved.

Our review of the literature showed that all functional schemes of electrostatic field strength meters use a current-to-voltage conversion unit. A typical solution for the implementation of which is the use of a differential TIA, which causes the main component of the instrumental measurement error. The shortcoming of the above works is that there are partially or completely missing data on the effect of differential TIA on the measurement error. And in the studies that give the numerical value of the total measurement error, the share of influence or the value of the error caused by the use of differential TIA is not indicated. Therefore, there is a need to establish the numerical value of the instrumental measurement error, which is caused by the use of differential TIA, as well as to consider alternative methods in order to reduce it.

All this gives reason to assert that it is expedient to conduct a study aimed at improving the method of converting the current received from the sensor into voltage, which would reduce the instrumental measurement error and ensure stability.

## 3. The aim and objectives of the study

The purpose of this study is to increase the accuracy of measuring the strength of electrostatic fields by reducing the instrumental measurement error caused by the use of differential transimpedance amplifiers. Conducting these studies could make it possible to establish the optimal current-to-voltage scheme, which would increase the sensitivity of the EFM sensor.

To achieve the goal, the following tasks were set:

– to justify the criteria for choosing the optimal OAs for building a TIA scheme;

– to analyze the criteria for choosing the optimal OAs and the selection of a set of available OAs of various models that meet the established criteria;

– to conduct computer simulations of circuits in order to study noise parameters in the frequency range of 10 Hz–10 MHz;

– to carry out computer simulations of the stability of the amplification factor of the circuits depending on the various ranges of input currents.

## 4. The study materials and methods

The object of our research is the process of measuring the strength of the electrostatic field. The subject of the study is the conversion of the current obtained from the sensor of the electrostatic field mill into voltage, which will reduce the instrumental error and ensure the linearity of the measurement of the atmospheric electrostatic field intensity.

The main hypothesis of the research assumes that the designed authentic circuit of an ungrounded differential transimpedance amplifier with zero voltage drop has better parameters of linearity and noise immunity, in contrast to the generally accepted one. The current article discusses the aspects of using TIA for the task of converting the current received from the EFM sensor into voltage, which can contribute to the improvement of hardware and the reduction of errors in measuring the strength of the atmospheric electrostatic field.

An electrostatic field mill works by moving a grounded shield plate over the electrode sensor plates, alternately exposing the sensor plates to an electric field and then shielding them. This alternation can be continuous, using a grounded rotor that rotates with an angular frequency ω, or due to the movement of the shielding plate back and forth [4, 12]. The surrounding electric field, which changes at a speed lower than the rotation speed of EFM, induces a current whose amplitude is directly proportional to the magnitude of the field strength. The signal from the sensor plate reaches the TIA, which converts the input current into voltage.

Transimpedance amplifiers are widely used to convert the current output of sensors, such as photodiode signals, into voltage signals that can be measured with minimal uncertainties. An operational amplifier with a feedback resistor from the output to the inverted input is the simplest implementation of such a TIA. However, even this simple TIA scheme requires a careful trade-off between noise gain, bias voltage, and self-excitation immunity. It is obvious that stability in TIA is important for reliable operation [18–22].

The generalized view of the sensor is shown in Fig. 1. In the study, an increase in the sensitivity of the EFM sensor was proposed due to the differential inclusion of the sensor plates. This implementation is possible when using an even number of vanes (sectors) of the EFM sensor since the amplitude of the signal from the group of sensor plates A will always be in antiphase with the group B (Fig. 1). This is due to the fact that at a certain point in time, a group of plates A is directly under the direct action of an electrostatic field, and an electric charge is induced on them. While the group of sensor plates B is shielded, the charge accumulated on them flows to the ground. When rotating the screen to the next sector, groups of plates A and B change their state to the opposite. Due to the rotating movement of the rotor, this change of states is cyclic.

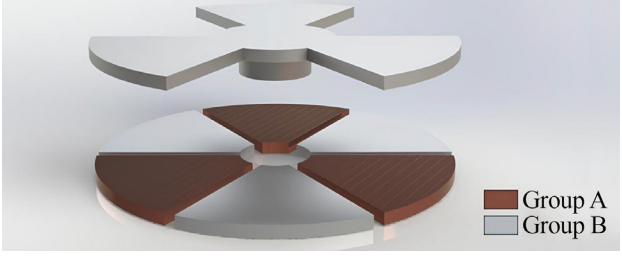


Fig. 1. Generalized view of the sensor plate, consisting of 6 sectors connected in 2 groups (groups A and B, marked with corresponding colors)

Accordingly, in order to receive data from the sensor in a configuration with differential switching on of the plates, it is necessary to change the switching type of the amplifier.

During the first stage of the research, aimed at establishing the optimal current measurement scheme from the EFM sensor, an analysis of the features of the topologies of TIA was carried out. Two TIA schemes were chosen for the study, shown in Fig. 2.

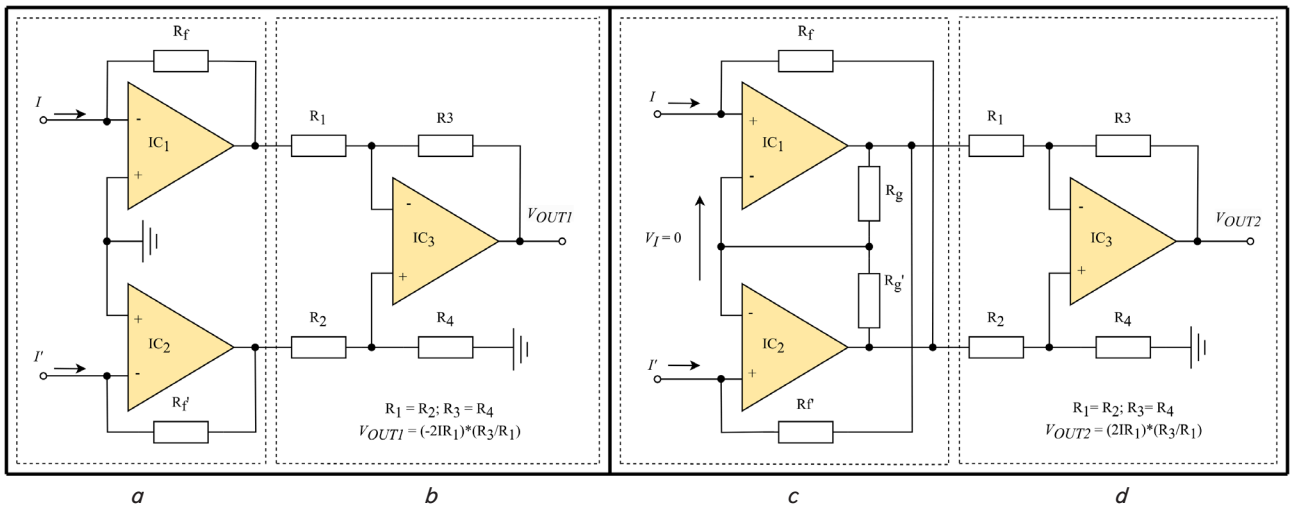


Fig. 2. Schemes of a differential transimpedance amplifier: *a*, *b* — a typical scheme; *c*, *d* — scheme of an ungrounded differential transimpedance amplifier with zero voltage drop

It is assumed that the circuit of the differential transimpedance amplifier (Fig. 2, *a*, *b*) will have the working name TP1, and the circuit of the ungrounded differential transimpedance amplifier with zero voltage drop (Fig. 2, *c*, *d*) will have the working name TP2. The TP1 scheme consists of two components: TIA (*a*) and a differential amplifier (*b*), and the TP2 scheme consists of an ungrounded current meter with a low voltage drop (*c*) and a differential amplifier (*d*). Since the differential amplifier (Fig. 2, *b*, *d*) is a common element for circuits TP1 and TP2, its structure will be considered last.

First, the structure of TP1 was considered. This circuit is based on two TIA circuits (Fig. 2, *a*), which convert the currents from the group of plates A and B, respectively. The transimpedance circuit configuration of the operational amplifier converts the input current source to the output voltage. The current-to-voltage gain is based on the feedback resistance $R_f$; as the usable signal is applied to the inverting inputs, the value of the output voltage $V_{out}$ is described by the following equation:

$$V_{out} = -2I \cdot R_f. \quad (1)$$

In turn, TP2 is implemented on the basis of an electrometric subtractor circuit, the feedback resistors of which are included in opposite feedback circuits. The amplification of this circuit will differ from TP1 only in sign since the usable signal is applied to non-inverting inputs:

$$V_{out} = 2I \cdot R_f. \quad (2)$$

It is also worth noting that due to the presence of feedback in TP2 through resistors $R_g$ and $R'_g$, the potential at the non-inverting inputs of the circuit becomes equal to the value of the inverting inputs, which in turn are connected to each other. As a result, the potential difference between the inputs of two OAs is reduced to zero. This configuration almost completely eliminates the output voltage shift caused by the difference in OA parameters.

The main task of the differential amplifier is to amplify the voltage difference between the two inputs and extract the common-mode voltage. Input signals usually come from low-impedance sources because the input impedance of this circuit is determined by the resistive network. Given the equality of resistors $R_1=R_2$ and $R_3=R_4$, the gain of this circuit can be calculated as:

$$V_{out} = R_3 / R_1. \quad (3)$$

Another advantage of differential amplifiers is the ability to reduce the common-mode signal, which is known as the common-mode rejection ratio (CMRR). The value of CMRR is greatly affected by the difference in resistor ratings, so pre-qualifying resistors should be used to improve this parameter. Also, avoid placing capacitive loads directly at the amplifier output to minimize stability problems. Additional filtering can be done by adding capacitors in parallel with $R_3$ and $R_4$. When using large resistors, filtering will also improve the stability of the circuit.

Comparing expressions (1) and (2), it can be seen that TP1 and TP2 have gain coefficients equal in magnitude but opposite in sign. However, they fundamentally differ in input topology, which causes a difference in their stability, level of general noise, etc.

To study the schemes, it was necessary to first select a number of OAs that are most suitable according to the specified criteria. Thus, there was a need to substantiate and analyze the criteria for choosing optimal OAs for building a TA scheme.

The LTspice software of the Analog Devices company was used to analyze the TIA characteristics, which is a universal tool for designing and creating electrical circuits with an integrated mixed simulation simulator. This simulator makes it possible to perform a spectral analysis of the noise characteristics at the selected point of the scheme, as well as measure the noise characteristics given to the input.

## 5. Research results of differential transimpedance amplifier circuits

### 5. 1. Justification of the criteria for choosing the optimal operational amplifiers for building a circuit of transimpedance amplifiers

Bias current ($I_{bias}$) is an OA problem because it flows through the external resistance and creates a voltage that adds system errors. This is the leakage current that occurs at both inputs. Depending on the type of input transistor, the bias current can flow into or out of the input terminals.

The bias current of OA is a particularly important parameter during measurement, as the amount of $I_{bias}$ reduces the bus current supply to be measured, thereby causing a systematic error in the measurement. For the task of measuring small currents, $I_{bias}$ should be as small as possible. With large values of the feedback resistor, in the TIA circuit, the output voltage shift can numerically exceed the upper or lower supply limit, which in turn will lead to a complete loss of the usable signal.

Voltage noise ($e_n$) is a voltage fluctuation that has many components, of which two main ones should be distinguished: flicker noise and broadband noise (or white noise). Flicker noise usually starts at an angular frequency ($1/f$), which is mostly 1 kHz and increases linearly as it moves into the low frequency range with a slope of 3 dB. Accordingly, broadband noise is to the right of the angular frequency and is evenly distributed over the entire high-frequency range.

Current noise ($i_n$) has a much wider range of values than voltage noise, depending on the input structure of OA. This parameter is not always specified in the specification tables, but it can be calculated as the usual Schottky noise (or shot noise), which is caused by the bias current. Schematically, current noise can be represented as a noise source between inverting and non-inverting inputs. The input current noise density ($i_n$) is most often specified in the amplifier specification table in units of $fA{\cdot}Hz^{-1/2}$. Given that when measuring small currents, TIA circuits will have a very large nominal feedback resistor, the current noise parameter will have a dominant character.

The frequency that is the boundary between the end of the flicker noise and the beginning of the broadband noise is known as the angular frequency ($1/f$) and is a measure of the quality of OA. The angular frequencies $1/f$ are not necessarily the same for the voltage noise and current noise of a particular amplifier. In general, a current-feedback OA can have three $1/f$ angles: for voltage noise, inverting input current noise, and its non-inverting input current noise. In low-frequency measurements, flicker noise is the defining component of the total noise level, so the lower the $1/f$ frequency, the better.

The input bias voltage ($V_{OS}$) is defined as the voltage that must be applied between the two input terminals of OA in order to obtain zero volts at the output. The bias input voltage parameter is symbolically represented by a voltage source that is in series with the positive or negative inputs of the amplifier. The $V_{OS}$ parameter is considered a DC error and is present from the time the power is applied until it is turned off, with or without an input signal. This occurs during OA displacement, and its effect can only be reduced, not eliminated.

The cause of $V_{OS}$ is well known, mostly due to the inherent mismatch of input transistors and components during silicon die fabrication. The mismatch of the bias currents leads to a voltage difference at the input terminals of OA. The $V_{OS}$ parameter has been reduced thanks to modern manufacturing processes that have improved the matching of the input transistors.

Slew rate is the rate of change of the output voltage caused by a step change in the signal at the OA input. It is measured as a change in voltage over a certain time (units of measurement are V/μs or V/ms). Indicators of change in the rate of increase depend on the type of OA used. For high-gain input stages, there is a possibility that the signals may saturate, forcing the amplifier to act as a DC source. When this happens, the rate of change of the amplifier's output signal is severely limited. The speed of increase is determined by the characteristics and internal structure of the OA microcircuit, so this parameter should be taken into account when designing new circuits.

Open-loop DC gain ($A_{VOL}$) is the inherent gain of an amplifier without closed-loop feedback. Open-loop gain is not a precisely controlled specification. It has a relatively large range and, in most cases, will be given in the specifications as a typical value. This parameter is very important in calculations because signal amplification and noise amplification depend on its value. The classic expression for calculating the gain of a closed-loop amplifier assumes the gain of an open circuit:

$$G = \frac{N_G}{1 + \frac{N_G}{A_{VOL}}}, \tag{4}$$

where $G$ is the actual OA gain, $N_G$ is the noise gain, and $A_{VOL}$ is the open-loop gain of the amplifier. From expression (4), it can be concluded that with a small value of $A_{VOL}$, the gain of the closed circuit will be less than the gain of the noise, accordingly, the signal-to-noise ratio (*SNR*) will deteriorate. Therefore, to improve the *SNR* value, it is necessary to choose an OA with a very high open-loop gain.

The input impedance ($R_{IN}$) of OA is an important factor in the design of any circuit, as is the output impedance ($R_{OUT}$). The $R_{IN}$ parameter determines the level of reduction of the input voltage due to the formation of a voltage divider. In turn, the $R_{OUT}$ parameter determines the voltage drop in the OA itself, which causes power dissipation. A large resistance limits the output power of the OA, and when an unbalanced load is turned on at the output, it serves as a voltage divider. When designing circuits sensitive to small currents, it is important that the $R_{IN}$ value be as large as possible to minimize current leakage to ground. And the value of $R_{OUT}$ as small as possible to reduce errors caused by temperature drift and amplitude losses between stages.

### 5. 2. Analysis of criteria for choosing optimal operational amplifiers for the construction of transimpedance amplifier circuits

The following OA selection criteria and their priority according to the degree of influence on the sensitivity of the TIA scheme have been determined:

1. To build a sensitive TIA circuit, the bias current ($I_{bias}$) was determined as the main OA parameter, because it has a very wide range of values among different OAs, and it is this that determines the minimum current that the amplifier can accept.

2. The current noise parameter ($i_n$) was chosen as the second priority because it will be the main component of the total noise since it will acquire the same gain as the usable signal. Therefore, when choosing a microcircuit, preference was given to the OA with the minimum parameter $i_n$ and the minimum parameter of the angular frequency $i_{nk}$.

3. To minimize the difference in signal gain and noise, it was customary to choose microcircuits with a large value of the $A_{VOL}$ parameter, a large input resistance $R_{IN}$ and a small output resistance $R_{OUT}$.

4. Since the TIA scheme involves a large amplification factor, special attention was paid to the Slew rate parameter since the discrepancy between the steepness of the output signal and the slew rate will lead to its distortion.

5. The parameters of the input voltage offset $V_{OS}$ and voltage noise $e_n$ are not decisive for this circuit, but are also components of measurement errors, so the value of these parameters should also be minimal.

The list of OA components and their characteristics are given in Table 1.

Table 1

List of components and their noise characteristics

| No. | Component name | $A_{VOL}$, dB | Slew Rate, V/uS | $V_{OS}$, uV | $e_n$, nV/Hz$^{1/2}$ | $e_{nk}$, Hz | $i_n$, fA/Hz$^{1/2}$ | $i_{nk}$, Hz | $R_{IN}$, Ω | $R_O$, Ω | $I_{bias}$, pA |
|---|---|---|---|---|---|---|---|---|---|---|---|
| 1 | LTC6268-10 | 106 | 1000 | 200 | 4 | 1M | 7 | 100k | 1T | 100 | 0.03 |
| 2 | MAX9636 | 130 | 0.9 | 300 | 38 | 1k | 0.9 | 10 | 500M | 1k | 0.1 |
| 3 | MAX40110 | 120 | 7 | 30 | 12.7 | 10k | 1.2 | 10k | 1T | 500 | 1 |
| 4 | OAA381 | 135 | 12 | 7 | 10 | 1M | 20 | 10k | 10T | 1k | 3 |
| 5 | TLE2037A-Q1 | 105.6 | 2.8 | 10 | 2.5 | 1k | 800 | 1k | 500M | 50 | 15k |
| 6 | LMP7731 | 130 | 2.4 | 9 | 3 | 1k | 1100 | 1k | 151M | 1k | 30k |
| 7 | AD797 | 86 | 20 | 10 | 0.9 | 1k | 2000 | 1k | 100M | 0.3m | 80k |

On the basis of justified criteria and our analysis, a number of OAs of different models, listed in Table 1, were selected for building TIA schemes and conducting computer simulations.

**5. 3. Results of computer simulation of circuit noise parameters in the frequency range**

The next stage of the research was to conduct computer simulations of the actual amplification factor for both TIA schemes. This chapter reports the results of our simulations of circuit noise parameters in the frequency range.

To analyze the circuits, the optimal amplification parameters were set, because when a large resistance was set in the feedback, some of the amplifiers lost their stability and went into the self-excitation mode, in which they generated high-frequency fluctuations.

The total noise parameter was measured as the rms noise level in the range from 10 Hz to 10 MHz. The measurements were performed without using filtering to calculate the intrinsic noise of the circuits. Fig. 3 shows an example of a chart of the distribution of noise density $e_n$ (in units of V/Hz$^{1/2}$) versus the frequency $f$ (in Hz) for the MAX9636 microcircuit.

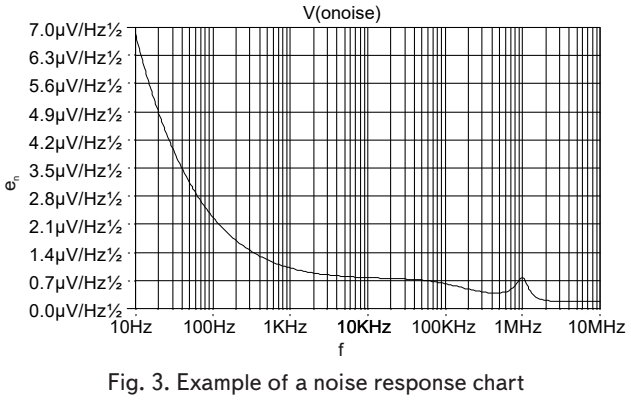


Fig. 3. Example of a noise response chart for a MAX9636 chip

To check the immunity of the scheme, a computer simulation was carried out, in which a signal with an amplitude of 10 pA was converted into a voltage with an amplification factor of $10^{10}$ times. The obtained values of the signal amplitude (*Amp*), the root mean square value of the noise (*Noise*) and their signal-to-noise ratio (*SNR*) expressed in decibels for both schemes in accordance with the simulated component are given in Table 2.

According to the results obtained during computer simulation, the noise characteristics given in Table 2, it can be argued that the TP2 scheme has better noise immunity than TP1, and the *SNR* value has improved by 42 % on average. The best result was obtained for the MAX40110 chip, for which the *SNR* ratio increased by 111.6 %. Separately, it is worth noting the LMP7731 microcircuit, which showed the best *SNR* values among the proposed OAs when using the TP2 circuit.

Table 2

Results of simulation of TP1 and TP2 schemes

| $I$=10 pA | | TP 1 | | | TP 2 | | |
|---|---|---|---|---|---|---|---|
| No. | Component name | *Amp*, mV | *Noise*, mV | *SNR*, dB | *Amp*, mV | *Noise*, mV | *SNR*, dB |
| 1 | LTC6268-10 | 99.5 | 2.1375 | 33.36 | 99.6 | 2.14 | 33.36 |
| 2 | MAX9636 | 99.4 | 1.035 | 39.65 | 99.5 | 0.726 | 42.74 |
| 3 | OAA381 | 99.6 | 3.1868 | 29.9 | 99.7 | 2.58 | 31.74 |
| 4 | MAX40110 | 99.6 | 1.7452 | 35.13 | 99.8 | 0.826 | 41.64 |
| 5 | TLE2037A-Q1 | 99.7 | 1.8518 | 34.62 | 99.7 | 1.75 | 35.11 |
| 6 | LMP7731 | 99.6 | 1.1262 | 38.93 | 99.7 | 0.636 | 43.9 |
| 7 | AD797 | 98.4 | 1.1016 | 39.02 | 98.9 | 0.83 | 41.52 |

**5. 4. Results of computer simulation of the stability of the amplification factor**

The next part of the study involved modeling the actual gain of the circuit, which was determined by studying the response of the circuit to different ranges of input currents at different gain ratios.

For the study, current was measured in the range from 1 pA to 1 uA because it is the most common among the amplitude range of EFM sensors. It was decided to divide this range of currents into three sub-ranges ([1 pA; 100 pA], [100 pA; 10 nA], [10 nA; 1 uA]), for a more detailed study of the characteristics of TIA circuits. Accordingly, for each range of currents, the optimal gain coefficients (10G, 100M and 1M) were selected, thus the resulting voltage at the output of each of the sub-ranges coincided with each other. In order to preserve the stability of TIA schemes, the amplification factor was evenly distributed between the cascades. Accordingly, the following circuit characteristics were selected for each sub-range of currents:

[1 pA; 100 pA]: $R_f$=2.5M; $R_1$=1k; $R_3$=1M;

[100 pA; 10 nA]: $R_f$=250k; $R_1$=1k; $R_3$=100k;

[10 nA; 1 uA]: $R_f$=25k; $R_1$=1k; $R_3$=10k.

Fig. 4 shows an example of the simulation results of the LTC6268-10 chip. As a result of the simulation, plots of the dependence of values of the actual gain (Gain) on the amplitude of the signal current *I*(*A*) were constructed, at different values of the feedback resistor, which demonstrate the linearity of the gain of TIA circuits.

From the constructed plots of the dependence of amplification factor on the value of the input signal, at different values of the feedback resistor (Fig. 4), it can be seen that:

1. The TP1 scheme has certain distortions of the amplification factor within [35 pA; 100 pA] at a factor of 10G (Fig. 4, *a*) and within [350 pA; 8 nA] at a factor of 100M (Fig. 4, *c*).

2. It is worth noting the good linearity in the range [1 pA; 35 pA] at a factor of 10G (Fig. 4, *a*).

3. Instead, the TP2 scheme has good linearity in a wide range of currents [100pA; 1uA] (Fig. 4, *d*, *e*), but the amplification factor becomes unstable at low current values [1 pA; 40 pA] and a large amplification factor of 10G (Fig. 4, *b*).

As a result of the analysis of our results of modeling the stability of amplification factor in different ranges of input currents ([1 pA; 100 pA], [100 pA; 10 nA], [10 nA; 1 uA]) at different amplification factors (10G, 100M and 1M) accordingly, it was established that the simulated amplification factor of the TP2 scheme is closer to the calculated value than that of TP1.

Thus, it can be asserted that the proposed TP2 scheme has better parameters of linearity and noise immunity in contrast to the generally accepted TP1.

Therefore, to increase the sensitivity of the EFM sensor in new devices, it will be effective to use the proposed scheme of an ungrounded differential transimpedance amplifier with zero voltage drop (TP2).

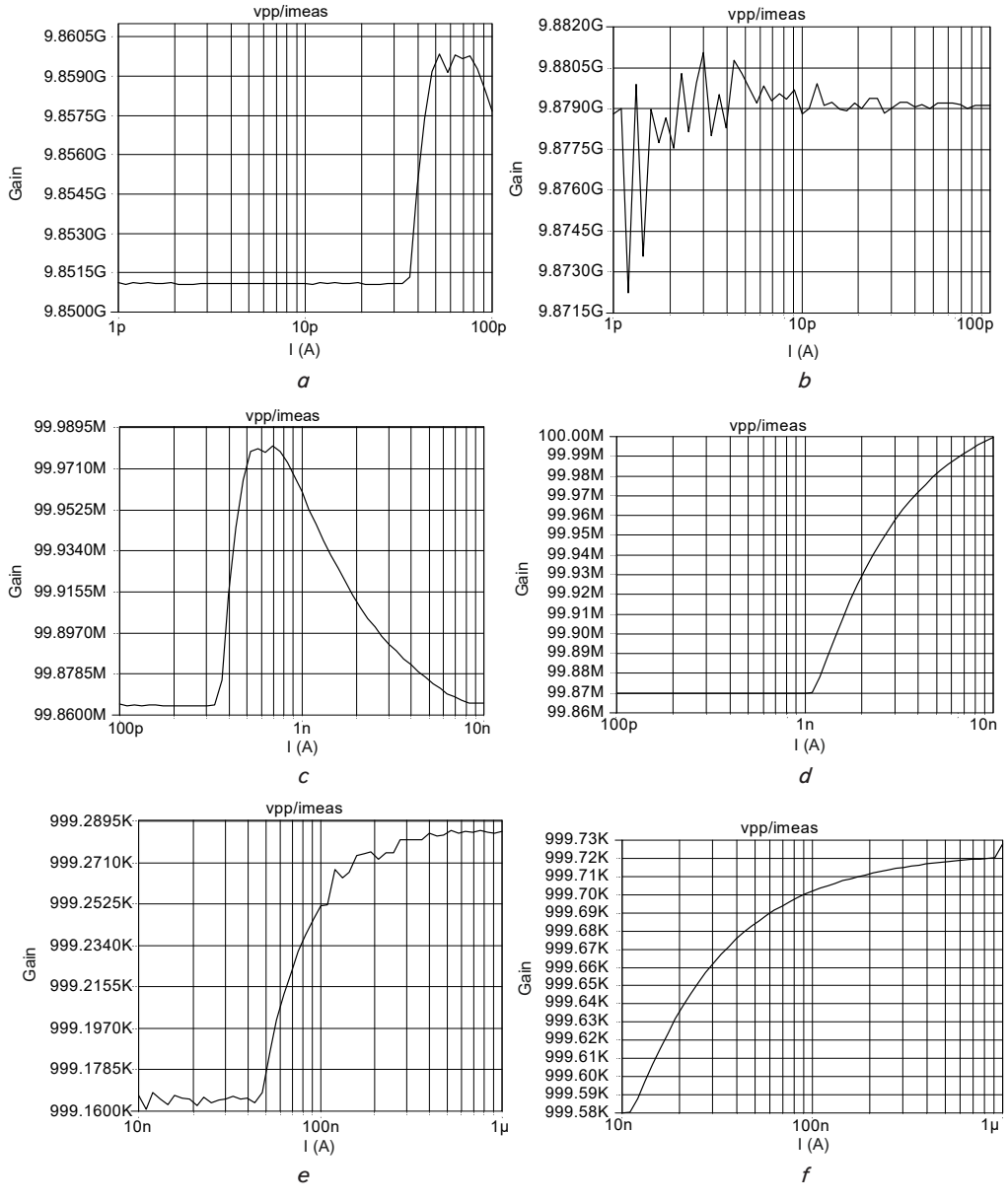


Fig. 4. Results of computer simulation of the stability of amplification factor (Gain) in different ranges of input currents and at different amplification factors: *a*, *b* — [1 pA; 100 pA], Gain=10G; *c*, *d* — [100 pA; 10 nA], Gain=100M; *e*, *f* — [10 nA; 1 uA], Gain=1M

## 6. Discussion of results of investigating the characteristics of differential transimpedance amplifiers for the tasks of measuring the strength of electrostatic fields

The main component of the EFM instrumental error occurs at the stage of converting current from the sensor into voltage. To minimize this error, it is necessary to conduct research and improve TIA circuits in order to increase the signal-to-noise ratio when measuring small current values. The comparative analysis of the typical scheme of the differential TIA reported in the current paper and the scheme of the ungrounded differential transimpedance amplifier with zero voltage drop (Fig. 2) that we proposed made it possible to establish the optimal current-to-voltage scheme.

In the work, the main result is the establishment of an optimal current-to-voltage conversion scheme for measuring small currents.

The practical application of our study could make it possible to increase the sensitivity of new devices for measuring the strength of the electrostatic field. In comparison with the existing scheme of differential TIA [6, 19], the proposed scheme of ungrounded differential TIA with zero voltage drop has better parameters of linearity (Fig. 2) and immunity (Table 2). The main advantage of the proposed scheme is that the stability of the gain is ensured, the influence of the bias parameters of the operational amplifier is leveled, and the overall noise level is reduced.

In contrast to study [6], in this paper, to demonstrate the effectiveness of the proposed EFM, the calculation of the inherent noise characteristics of the proposed scheme of an ungrounded differential TIA with zero voltage drop is given. An SNR parameter is also defined, with which the Effective Value of Bits (ENOB) parameter can be calculated. In contrast to [19], our study presents the noise characteristics of the proposed schemes of differential TIA, which will be used to calculate the total error of EFM.

One of the advantages of our research is the discussion of the priority of OA parameters according to the degree of their influence on the sensitivity of the TIA circuit, which will be useful when choosing a component base for building new devices. However, this research is limited to the use of computer simulations only and may differ from actual results. For the most part, this limitation is due to the imperfection of the mathematical models used by the software.

The main drawback of the current research is that the noise characteristics of only two schemes of differential TIA were analyzed. After all, there are other, less common schemes of differential TIAs that can also be used for tasks of measuring the intensity of electrostatic fields.

This research is focused on computer simulations of the proposed TIA scheme in order to investigate noise parameters in the frequency range of 10 Hz–10 MHz and the stability of the amplification factor depending on different ranges of input currents. However, future studies will include physical modeling of the proposed circuit of an ungrounded differential transimpedance amplifier with zero voltage drop, to experimentally confirm our results.

## 7. Conclusions

1. A comparative analysis of a typical circuit of a differential transimpedance amplifier (TP1) and a circuit of an ungrounded differential transimpedance amplifier with zero voltage drop (TP2) that we proposed was carried out. Combining expressions (1) and (2) with expression (3), it can be seen that TP1 and TP2 have gain coefficients equal in magnitude but opposite in sign. However, they fundamentally differ in input topology, which causes a difference in their stability, level of general noise, etc. During the first stage of the research, the criteria for choosing the optimal OAs for building the TIA scheme were substantiated.

2. An analysis of the criteria for choosing optimal OAs and the selection of a set of available OAs of various models that meet the established criteria were carried out. As a result of the analysis, it was determined that the bias current ($I_{bias}$) was defined as the main OA parameter for the construction of a sensitive TIA circuit. The current noise parameter ($i_n$) was chosen as the second priority. Also, to minimize the difference between signal gain and noise, it is determined that chips with a large value of $A_{VOL}$, a large input resistance $R_{IN}$, and a small output resistance $R_{OUT}$ should be selected. The slew rate parameter of OA must exceed the rise rate of the output signal, otherwise it can distort the waveform and prevent the true representation of the input signal at the output. It should be taken into account that the value of the parameters of the input voltage offset $V_{OS}$ and voltage noise $e_n$ should be minimal.

3. Computer simulations of the typical and proposed schemes were carried out in order to study noise parameters in the frequency range of 10 Hz–10 MHz. As a result, it was found that the TP2 scheme has better interference resistance than TP1, and the SNR value has improved by 42 % on average.

4. Computer simulations of the stability of amplification factor of the typical and proposed schemes were carried out depending on three ranges of input currents ([1 pA; 100 pA], [100 pA; 10 nA], [10 nA; 1 uA]) for different amplification factors (10G, 100M and 1M) respectively. It was established that the simulated amplification factor of the TP2 scheme is closer to the calculated value than that of TP1. It was established that the designed circuit of an ungrounded differential transimpedance amplifier with zero voltage drop has better parameters of linearity and immunity, unlike the generally accepted circuit for its use in order to measure the intensity of the atmospheric electric field.

## Conflicts of interest

The authors declare that they have no conflicts of interest in relation to the current study, including financial, personal, authorship, or any other, that could affect the study and the results reported in this paper.

## Funding

The study was conducted without financial support.

## Data availability

The data will be provided upon reasonable request.

## Use of artificial intelligence

The authors confirm that they did not use artificial intelligence technologies when creating the presented work.

References


1. Swenson, J. A., Beasley, W. H., Byerley, L. G., Bogoev, I. G. (2006). Pat. No. US7256572B2. Electric-field meter having current compensation. Available at: https://patents.google.com/patent/US7256572B2/en?oq=US+7.256%2c572
2. Slocum, C. D. (1976). Pat. No. US4095221A. Electrical storm forecast system. Available at: https://patents.google.com/patent/US4095221A/en?oq=US+4%27095%27221
3. Wells, T. J., Elliott, R. S. (2003). Pat. No. US6982549B1. Micro-electrometer. Available at: https://patents.google.com/patent/US6982549B1/en?oq=US+6%27982%27549
4. Antunes de Sá, A., Marshall, R., Sousa, A., Viets, A., Deierling, W. (2020). An Array of Low-Cost, High-Speed, Autonomous Electric Field Mills for Thunderstorm Research. Earth and Space Science, 7 (11). doi: https://doi.org/10.1029/2020ea001309
5. Yamashita, K., Fujisaka, H., Iwasaki, H., Kanno, K., Hayakawa, M. (2022). A New Electric Field Mill Network to Estimate Temporal Variation of Simplified Charge Model in an Isolated Thundercloud. Sensors, 22 (5), 1884. doi: https://doi.org/10.3390/s22051884
6. Wilson, J. G., Cummins, K. L. (2021). Thunderstorm and fair-weather quasi-static electric fields over land and ocean. Atmospheric Research, 257, 105618. doi: https://doi.org/10.1016/j.atmosres.2021.105618
7. Emersic, C., Saunders, C. P. R. (2020). The influence of supersaturation at low rime accretion rates on thunderstorm electrification from field-independent graupel-ice crystal collisions. Atmospheric Research, 242, 104962. doi: https://doi.org/10.1016/j.atmosres.2020.104962
8. Korovin, E. A., Gotyur, I. A., Kuleshov, Y. V., Shchukin, G. G. (2019). Lightning discharges registration by the electric field mill. IOP Conference Series: Materials Science and Engineering, 698 (4), 044047. doi: https://doi.org/10.1088/1757-899x/698/4/044047
9. Chubb, J., Harbour, J. (2010). 'Operational health' monitoring for confidence in long term electric field measurements. Journal of Electrostatics, 68 (5), 469–472. doi: https://doi.org/10.1016/j.elstat.2010.07.001
10. Cui, Y., Yuan, H., Song, X., Zhao, L., Liu, Y., Lin, L. (2018). Model, Design, and Testing of Field Mill Sensors for Measuring Electric Fields Under High-Voltage Direct-Current Power Lines. IEEE Transactions on Industrial Electronics, 65 (1), 608–615. doi: https://doi.org/10.1109/tie.2017.2719618
11. Bateman, M. G., Stewart, M. F., Podgorny, S. J., Christian, H. J., Mach, D. M., Blakeslee, R. J. et al. (2007). A Low-Noise, Microprocessor-Controlled, Internally Digitizing Rotating-Vane Electric Field Mill for Airborne Platforms. Journal of Atmospheric and Oceanic Technology, 24 (7), 1245–1255. doi: https://doi.org/10.1175/jtech2039.1
12. Povcshenko, O., Bazhenov, V. (2023). Analysis of modern atmospheric electrostatic field measuring instruments and methods. Technology Audit and Production Reserves, 4 (1 (72)), 16–24. doi: https://doi.org/10.15587/2706-5448.2023.285963
13. Chu, Z., Peng, C., Ren, R., Ling, B., Zhang, Z., Lei, H., Xia, S. (2018). A High Sensitivity Electric Field Microsensor Based on Torsional Resonance. Sensors, 18 (1), 286. doi: https://doi.org/10.3390/s18010286
14. Lemonou, A., Agorastou, Z., Noulis, T., Siskos, S. (2022). Low Noise-Low Power Transimpedance Amplifier Design for Electric Field Sensing. 2022 Panhellenic Conference on Electronics & Telecommunications (PACET). doi: https://doi.org/10.1109/pacet56979.2022.9976379
15. Agorastou, Z., Noulis, T., Siskos, S. (2022). Analog Sensor Interface for Field Mill Sensors in Atmospheric Applications. Sensors, 22 (21), 8405. doi: https://doi.org/10.3390/s22218405
16. Agorastou, Z., Michailidis, A., Lemonou, A., Themeli, R., Noulis, T., Siskos, S. (2023). Integrated Filter Design for Analog Field Mill Sensor Interface. Sensors, 23 (7), 3688. doi: https://doi.org/10.3390/s23073688
17. Bazhenov, V., Povcshenko, O. (2023). Methodological features of calculating errors in the measurement of electrostatic field strength. Bulletin of Kyiv Polytechnic Institute. Series Instrument Making, 65 (1), 65–72. doi: https://doi.org/10.20535/1970.65(1).2023.283358
18. Demirtaş, M., Erişmiş, M. A., Güneş, S. (2020). Analysis and design of a transimpedance amplifier based front-end circuit for capacitance measurements. SN Applied Sciences, 2 (2). doi: https://doi.org/10.1007/s42452-020-2104-x
19. Noh, J.-H. (2020). Frequency-Response Analysis and Design Rules for Capacitive Feedback Transimpedance Amplifier. IEEE Transactions on Instrumentation and Measurement, 69 (12), 9408–9416. doi: https://doi.org/10.1109/tim.2020.3006325
20. Thandri, B. K., Silva-Martinez, J. (2006). An overview of feed-forward design techniques for high-gain wideband operational transconductance amplifiers. Microelectronics Journal, 37 (9), 1018–1029. doi: https://doi.org/10.1016/j.mejo.2006.02.003
21. Rezaei, I., Khani, A. A. M., Dadgar, M., Attar, M. (2023). Fully active frequency compensation analysis on multi-stages CMOS amplifier. Memories - Materials, Devices, Circuits and Systems, 5, 100068. doi: https://doi.org/10.1016/j.memori.2023.100068
22. Bendre, V. S., Kureshi, A. K. (2017). An Overview of Negative Feedback Compensation Techniques for Operational Transconductance Amplifiers. 2017 International Conference on Computing, Communication, Control and Automation (ICCUBEA). doi: https://doi.org/10.1109/iccubea.2017.8463683